AlInAsSb Impact Ionization Coefficients

Yuan Yuan[®], Jiyuan Zheng[®], Ann K. Rockwell[®], Stephen D. March, Seth R. Bank, and Joe C. Campbell[®]

Abstract—Digital alloy AlInAsSb avalanche photodiodes exhibit low excess noise comparable to those fabricated from Si. The electron and hole ionization coefficients are critical parameters for simulation and analysis of high-sensitivity receivers. We report ionization coefficients using a mixed injection technique that employs measurement of the gain for different incident wavelengths and a simulation algorithm.

 ${\it Index Terms} {\bf -Avalanche \ \ photodiodes, \ \ impact \ \ ionization, absorption \ coefficient.}$

THE internal gain of avalanche photodiodes (APDs) enables high receiver sensitivity, which has resulted in their wide deployment in long-haul optical communication systems, three-dimensional imaging cameras, a wide range of sensing applications, light detection and ranging (LIDAR) and data centers. However, the stochastic nature of the multiplication mechanism, impact ionization, results in gain fluctuations, a source of noise that is typically expressed as a multiplicative factor, F(M), in the shot noise, which becomes [1], [2]:

$$\langle i_{shot}^2 \rangle = 2q (I_{photo} + I_{dark}) \langle M \rangle^2 F(M) \Delta f,$$
 (1)

where I_{photo} is photocurrent, I_{dark} is dark current, $\langle M \rangle$ is average gain, F(M) is referred to as the excess noise factor, and Δf is bandwidth. The tradeoff between the benefit of gain and the detriment of gain-linked noise is illustrated by the signal to noise ratio, SNR,

$$SNR = \frac{I_{photo}^2}{2qI_{total}F(M)\Delta f + \frac{\sigma_{circuit}^2}{M^2}},$$
 (2)

where $\sigma_{circuit}^2$ is the RMS noise current of the following electronic circuitry. The APD gain effectively suppresses the circuit noise until it reaches the point where the APD noise is comparable to that of the circuit. Thus it is beneficial to minimize F(M), which is a function of the average gain and k, the ratio of hole, β , to electron, α , ionization coefficients. For bulk multiplication regions where non-local effects can be ignored, the excess noise factor is given by F(M) = kM + (1-k)(2-1/M) [3]. The excess noise factor increases with increasing gain but increases more slowly the lower the

Manuscript received October 26, 2018; revised January 2, 2019; accepted January 15, 2019. Date of publication January 21, 2019; date of current version February 5, 2019. This work was supported in part by the Army Research Office under Grant W911NF-17-1-0065 and in part by DARPA under Grant GG11972.153060. (Corresponding author: Joe C. Campbell.)

Y. Yuan, J. Zheng, and J. C. Campbell are with the Electrical and Computer Engineering Department, University of Virginia, Charlottesville, VA 22904 USA (e-mail: jcc7s@virginia.edu).

A. K. Rockwell, S. D. March, and S. R. Bank are with the Electrical and Computer Engineering Department, University of Texas at Austin, Austin, TX 78758 USA.

Color versions of one or more of the figures in this letter are available online at http://ieeexplore.ieee.org.

Digital Object Identifier 10.1109/LPT.2019.2894114

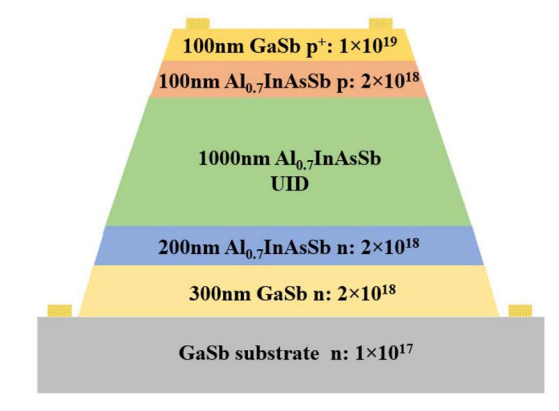


Fig. 1. Schematic cross section of Al_{0.7}InAsSb p-i-n APD.

value of k. This reinforces the importance of determining the ionization coefficients and understanding the mechanisms that suppress or enhance one relative to the other [4]–[6].

Recently, APDs fabricated from $Al_xIn_{1-x}As_ySb_{1-y}$ digital alloys lattice-matched to GaSb [7]–[11] and $In_{0.52}Al_{0.48}As$ digital alloy on InP [12]–[14] have exhibited very low excess noise, comparable to that of Si. Since these are direct bandgap materials and thus have shorter absorption lengths than indirect materials such as Si, they have the potential for high speed owing to shorter transit times. In addition, the $Al_xIn_{1-x}As_ySb_{1-y}$ digital alloy can operate across a wide spectral range, from the near infrared through the mid-wave window, by tuning its composition.

In this letter, we report the optical characteristics: complex refractive indexes and absorption coefficients of Al_{0.7}In_{0.3}As_{0.3}Sb_{0.7} [referred to below as AlInAsSb] digital alloy by using spectroscopic ellipsometry. The multiplication gain characteristics and excess noise factors of the AlInAsSb digital alloy with different carrier injection profiles are also investigated. These data enable determination of the ionization coefficients of electrons and holes as functions of the electric field.

AlInAsSb layers were grown on n-type GaSb (001) substrates by solid-source molecular beam epitaxy (MBE). The layers use a digital alloy period of 10 monolayers (MLs) comprised of four binary alloys InAs, InSb, AlSb, and AlAs [15]. A cross-sectional schematic of the AlInAsSb p-i-n structure APD is shown in Fig. 1. From top to bottom, the structure consists a 100 nm GaSb p-type contact layer, a 100 nm AlInAsSb p-type layer, a 1000nm AlInAsSb UID multiplication layer, a 200 nm AlInAsSb n-type layer, a 300 nm GaSb n-type contact layer and an n-type GaSb substrate. The p-type and n-type layers are doped by Be and Te, respectively.

The mesas were defined by standard photolithography and formed by a combination of dry and wet etching to suppress surface dark current. Reactive ion etching (RIE) and

1041-1135 © 2019 IEEE. Personal use is permitted, but republication/redistribution requires IEEE permission. See http://www.ieee.org/publications_standards/publications/rights/index.html for more information.

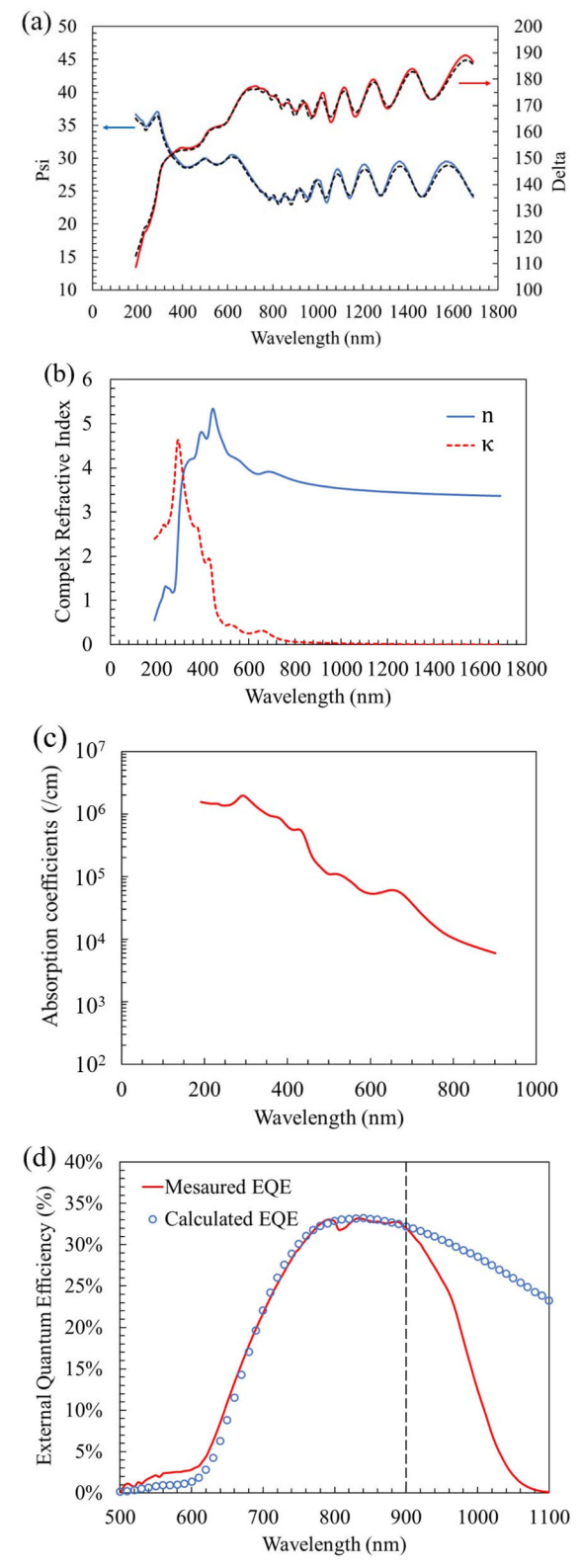


Fig. 2. Optical characteristics of Al_{0.7}InAsSb digital alloy as measured with spectroscopic ellipsometry: (a) reflection parameters versus wavelength, (b) complex refractive index, and (c) absorption coefficient versus wavelength. (d) Meausred and calculated external quantum efficiencies of Al_{0.7}InAsSb digital alloy.

inductively coupled plasma (ICP) were used to etch approximately $1\mu m$. The mesa etch was completed with a critic acid solution. Ti/Au was deposited as the top and bottom contacts by electron-beam evaporation.

The optical characteristics of AlInAsSb digital alloy were measured by spectroscopic ellipsometry. Ellipsometry measures two values, Ψ and Δ , the amplitude ratio and phase difference between p-polarized and s-polarized light waves, respectively. The complex reflectance ratio, ρ , is given by the expression [16]:

$$\rho = \tan(\Psi)e^{i\Delta}.\tag{3}$$

The measured Ψ and Δ values at 60° incidence angle are shown in Fig. 2 (a), where the solid lines are the measured reflection values using Eq. (3), and the dash lines are fitted curves. Here, the optical properties of the AlInAsSb layers are approximated by effective medium approximations (EMA) with the Burggeman analysis technique [17]. We note that the thickness of the top GaSb cap layer and its optical parameters are well known. The model can decouple GaSb and AlInAsSb thus eliminating the influence of the GaSb. Figure 2 (b) shows the real part, n, and the imaginary part, κ , of the deduced digital alloy AlInAsSb complex refractive index. The absorption coefficients versus wavelength are plotted in Fig. 2 (c). The measured external quantum efficiency (solid line) and the calculated efficiency ("O" data points) using the absorption coefficients are shown in Fig. 2 (d). They agree for wavelengths up to \sim 900 nm.

The multiplication gain measurements of the AlInAsSb APD are shown in Fig. 3. The different wavelength lasers permit gain measurements corresponding to diverse carrier injection profiles. To determinate the ionization coefficients, the typical experimental measurement technique is based on pure electron and pure hole initiated multiplication [18]. However, in the absence of pure carrier injection, any two sets of gain measurements with known injection profiles can be used to obtain reliable ionization coefficients. Compared to the mixed injection method, the pure carrier injection method requires fully symmetrical p-i-n and n-i-p APDs, or top and back illumination, which may, at times, be limited by material and processing issues.

In Fig. 3, the multiplication gain curves at 543 nm, 633 nm, and 850 nm provide three different injection profiles that can be used to determined the ionization coefficients. The gain curves move to higher bias voltages at longer illuminated wavelength, which indicates that the electron ionization coefficient, α , is larger than the hole ionization coefficient, β [19], [20].

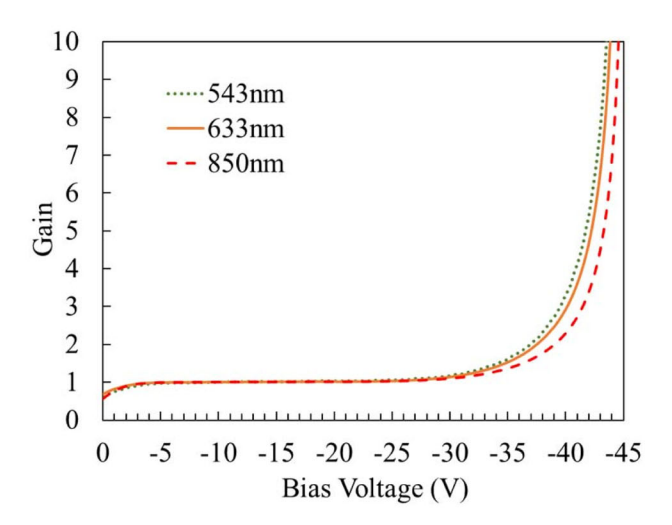
Excess noise factor characteristics, F(M), for AlInAsSb digital alloy APD, again achieved at 543 nm, 633 nm, and 850 nm wavelengths, are plotted in Fig. 4. The excess noise factors measured at 543 nm laser are the lowest, since this wavelength produces pure electron injection. As the wavelength increases, there are more holes injected into the multiplication region, and the excess noise factor increases. This tendency is consistent with the conclusion that α is larger than β .

The mixed injection multiplication gain can be calculated using the following expressions [21], [22]:

$$M_{mix} = \frac{\int_0^W M(x)G(x)dx}{\int_0^W G(x)dx},\tag{4}$$

TABLE I
ABSORPTION COEFFICIENTS AND ABSORPTION PERCENTAGES OF DIFFERENT LAYERS

Layers	543 nm (μm ⁻¹)	Absorption @ 543 nm	633 nm (μm ⁻¹)	Absorption @ 633 nm	850 nm (μm ⁻¹)	Absorption @ 850 nm
GaSb (p-type, 100nm)	41.21	69%	23.66	63%	4.42	25%
Al _{0.7} InAsSb (p-type, 100nm)	9.26	1%	5.82	3%	0.77	3%
Al _{0.7} InAsSb (UID, 1000nm)	9.26	0	5.82	4%	0.77	22%
Al _{0.7} InAsSb (n-type, 200nm)	9.26	0	5.82	0	0.77	3%
GaSb (n-type, 300nm)	41.21	0	23.66	0	4.42	12%



Multiplication gain versus voltage of an Al_{0.7}InAsSb digital alloy APD.

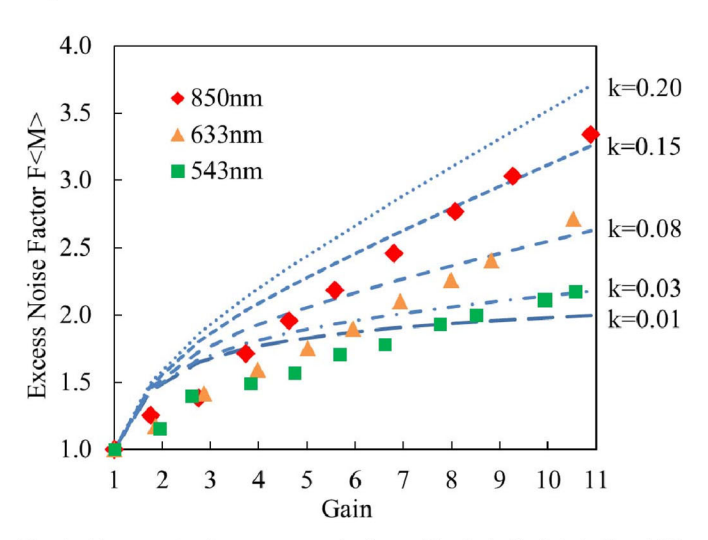


Fig. 4. Excess noise factor versus gain for an Al_{0.7}InAsSb digital alloy APD.

$$G(x) \propto e^{-\gamma x},$$
 (5)

$$G(x) \propto e^{-\gamma x}, \tag{5}$$

$$M(x) = \frac{(\alpha - \beta)e^{-(\alpha - \beta)x}}{\alpha e^{-(\alpha - \beta)W} - \beta}, \tag{6}$$

where W is depletion region width, γ is absorption coefficient, G(x) is the carrier generation rate, and M(x) is the gain for an electron-hole pair injected at position x. By using the

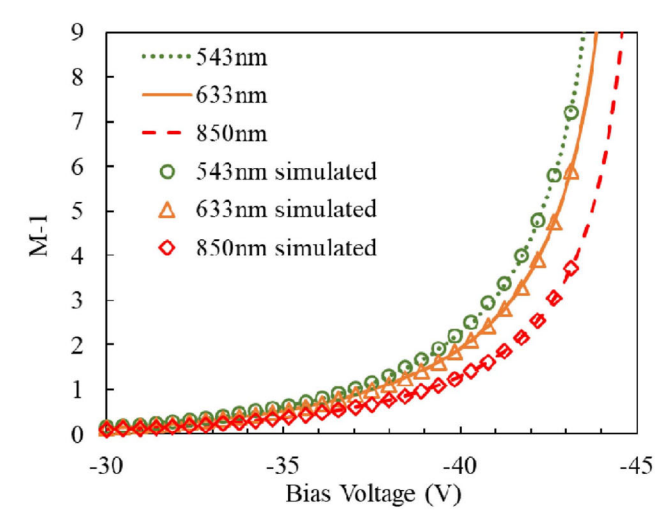


Fig. 5. Measured (lines) and simulated (symbols) multiplication gain curves of an Al_{0.7}InAsSb digital alloy APD.

equations above and the three wavelength multiplication gain sets, the ionization coefficients can be simulated. It can be seen in Fig. 3 that the avalanche gain starts at approximately -30 V. Figure 5 shows good agreement between the simulated gain and the measured gain values.

Combined with the absorption coefficients for each layer, these simulated gain values can be used to deduce the ionization coefficients of the AlInAsSb digital alloy. The absorption coefficients determined from the data in Fig. 2 (c) and the light absorption percentages in each layer (considered 30% reflection at the interface between air and top GaSb layer) are shown in table I.

The electric field calculation includes the built-in voltage, which can be calculated as: $V_{bi} = (k_B T/q) \times \ln(N_d N_a/n_i^2)$, where $n_i = \sqrt{N_C N_V} \times \exp\left(-E_g/2k_BT\right)$, $E_g \sim 1.13 \mathrm{eV}$, and N_C , N_V were estimated using the parameters for $Ga_xInAsSb$ [23]: $N_C = 2.5 \times 10^{19} \times (0.022 + 0.03x - 0.012x^2)^{3/2}$, $N_V = 2.5 \times 10^{19} \times (0.41 + 0.16x + 0.23x^2)^{3/2}$, with x = 0.7. Here V_{bi} is approximately 1.14 V. To assess the accuracy of the simulated results, the α (\bigcirc) and β (\triangle) determined from pure carrier injection by measuring the gain of p-i-n and n-i-p APDs [24] are also plotted in Fig. 6. The ionization coefficients simulated using the mix injection method are in good agreement with the results obtained from pure carrier injection. The agreement also supports the absorption coefficients of the

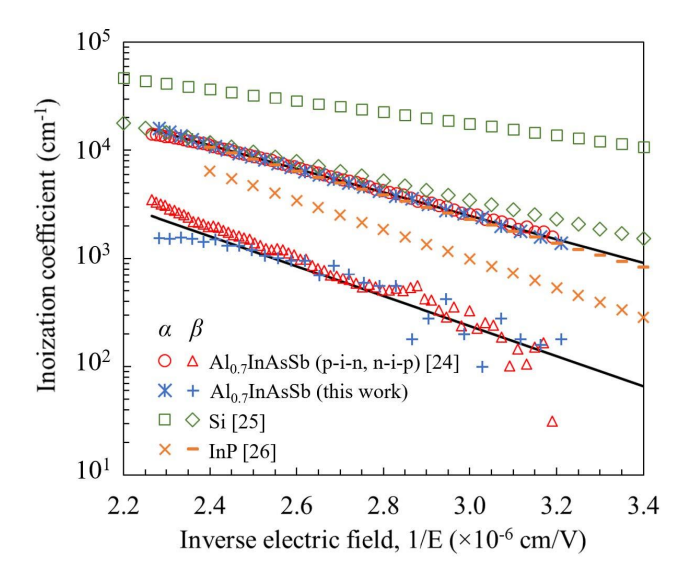


Fig. 6. Ionization coefficients of the Al_{0.7}InAsSb determined using the pure carrier injection method [26] and the mix injection method. The ionization coefficients of Si [27] and InP [28] are shown for comparison.

AlInAsSb digital alloy. The results of this study can be used to generate the following analytical expressions for the ionization coefficients, which are plotted as solid lines in Fig 6:

$$\alpha(E) = 4.5 \times 10^6 \times \exp(-2.5 \times 10^6/E),$$
 (7)

$$\beta(E) = 3.5 \times 10^6 \times \exp(-3.2 \times 10^6 / E).$$
 (8)

The ionization coefficients of Si [25] and InP [26] are also plotted in Fig. 6 for comparison. The AlInAsSb APD has comparable low excess noise to that of Si and both materials exhibit α/β ratios that are much larger than InP.

In conclusion, the complex refractive indices and the absorption coefficients from 500 nm to 900 nm of the AlInAsSb digital alloy have been determined. The mixed injection technique has been used to determine the ionization coefficients. The results are consistent with measurements obtained by pure carrier injection with p-i-n and n-i-p AlInAsSb APDs.

REFERENCES

- [1] J. C. Campbell, "Recent advances in avalanche photodiodes," *J. Lightw. Technol.*, vol. 34, no. 2, pp. 278–285, Jan. 15, 2016.
- [2] J. C. Campbell, "Advances in photodetectors," in *Optical Fiber Telecommunications Part A: Components and Subsystems*, vol. 5, I. Kaminow, T. Li, and A. E. Wilner, Eds., 5th ed. New York, NY, USA: Academic, 2008.
- [3] R. J. McIntyre, "Multiplication noise in uniform avalanche diodes," IEEE Trans. Electron Devices, vol. ED-13, no. 1, pp. 164–168, Jan. 1966.
- [4] J. Zheng et al., "A PMT-like high gain avalanche photodiode based on GaN/AlN periodically stacked structure," Appl. Phys. Lett., vol. 109, no. 24, p. 241105, 2016.

- [5] J. Zheng et al., "Theoretical study on interfacial impact ionization in AlN/GaN periodically stacked structure," Appl. Phys. Express, vol. 10, no. 7, p. 071002, 2017.
- [6] J. Zheng et al., "The influence of structure parameter on GaN/AIN periodically stacked structure avalanche photodiode," IEEE Photon. Technol. Lett., vol. 29, no. 24, pp. 2187–2190, Dec. 15, 2017.
- [7] S. R. Bank et al., "Avalanche photodiodes based on the AlInAsSb materials system," *IEEE J. Sel. Topics Quantum Electron.*, vol. 24, no. 2, Mar./Apr. 2018, Art. no. 3800407.
- [8] M. Ren, S. J. Maddox, M. E. Woodson, Y. Chen, S. R. Bank, and J. C. Campbell, "Characteristics of Al_xIn_{1-x}As_ySb_{1-y} (X:0.3-0.7) avalanche photodiodes," *J. Lightw. Technol.*, vol. 35, no. 12, pp. 2380–2384, Jun. 15, 2017.
- [9] M. Ren, S. J. Maddox, M. E. Woodson, Y. Chen, S. R. Bank, and J. C. Campbell, "AlInAsSb separate absorption, charge, and multiplication avalanche photodiodes," *Appl. Phys. Lett.*, vol. 108, no. 19, p. 191108, 2016.
- [10] M. E. Woodson, M. Ren, S. J. Maddox, Y. Chen, S. R. Bank, and J. C. Campbell, "Low-noise AlInAsSb avalanche photodiode," *Appl. Phys. Lett.*, vol. 108, no. 8, p. 081102, 2016.
- [11] A.-K. Rockwell, Y. Yuan, A. H. Jones, S. D. March, S. R. Bank, and J. C. Campbell, "Al_{0.8}In_{0.2}As_{0.23}Sb_{0.77} avalanche photodiodes," *IEEE Photon. Technol. Lett.*, vol. 30, no. 11, pp. 1048–1051, Jun. 1, 2018.
- [12] Y. Yuan et al., "Temperature dependence of the ionization coefficients of InAlAs and AlGaAs digital alloys," *Photon. Res.*, vol. 6, no. 8, pp. 794–799, 2018.
- [13] J. Zheng et al., "Digital alloy InAlAs avalanche photodiodes," J. Lightw. Technol., vol. 36, no. 17, pp. 3580–3585, Sep. 1, 2018.
- [14] A. K. Rockwell *et al.*, "Toward deterministic construction of low noise avalanche photodetector materials," *Appl. Phys. Lett.*, vol. 113, no. 10, p. 102106, 2018.
- [15] S. J. Maddox, S. D. March, and S. R. Bank, "Broadly tunable AlInAsSb digital alloys grown on GaSb," *Cryst. Growth Des.*, vol. 16, no. 7, pp. 3582–3586, 2016.
- [16] H. Fujiwara, Spectroscopic Ellipsometry: Principles and Applications. Hoboken, NJ, USA: Wiley, 2007.
- [17] W. S. Weiglhofer, A. Lakhtakia, and B. Michel, "Maxwell Garnett and Bruggeman formalisms for a particulate composite with bianisotropic host medium," *Microw. Opt. Technol. Lett.*, vol. 15, no. 4, pp. 263–266, 1997.
- [18] F. Capasso, "Physics of avalanche photodiodes," Semicond. Semimetals, vol. 22, pp. 1–172, 1985.
- [19] X. Yi et al., "Demonstration of large ionization coefficient ratio in AlAs_{0.56}Sb_{0.44} lattice matched to InP," Sci. Rep., vol. 8, no. 1, 2018, Art. no. 9107.
- [20] J. Zheng et al., "Low-temperature-dependent property in an avalanche photodiode based on GaN/AlN periodically-stacked structure," Sci. Rep., vol. 6, Oct. 2016, Art. no. 35978.
- [21] G. E. Stillman and C. M. Wolfe, "Avalanche photodiodes," in *Semiconductors and Semimetals*, vol. 12, R. K. Willardson and A. C. Beer, Eds. New York, NY, USA: Academic, 1977, pp. 332–334.
- [22] J. S. Ng, C. H. Tan, J. P. R. David, G. Hill, and G. J. Rees, "Field dependence of impact ionization coefficients in In_{0.53}Ga_{0.47}As," *IEEE Trans. Electron. Devices*, vol. 50, no. 4, pp. 901–905, Apr. 2003.
- [23] [Online]. Available: http://www.ioffe.ru/SVA/NSM/Semicond/GaInAsSb/bandstr.html
- [24] Y. Yuan et al., "Comparison of different period digital alloy Al_{0.7}InAsSb avalanche photodiodes," J. Lightw. Technol., submitted for publication.
- [25] R. Van Overstraeten and H. De Man, "Measurement of the ionization rates in diffused silicon p-n junctions," *Solid-State Electron.*, vol. 13, no. 5, pp. 583–608, 1970.
- [26] L. W. Cook, G. E. Bulman, and G. E. Stillman, "Electron and hole impact ionization coefficients in InP determined by photomultiplication measurements," Appl. Phys. Lett., vol. 40, no. 7, pp. 589–591, 1982.